ACCELERATING HEP SIMULATIONS WITH NEURAL IMPORTANCE SAMPLING

Anonymous authors
Paper under double-blind review

ABSTRACT

Virtually all high-energy-physics (HEP) simulations for the LHC rely on Monte Carlo using importance sampling by means of the VEGAS algorithm. However, complex high-precision calculations have become a challenge for the standard toolbox. As a result, there has been keen interest in HEP for modern machine learning to power adaptive sampling. Despite previous work proving that normalizing-flow-powered neural importance sampling (NIS) sometimes outperforms VEGAS, existing research has still left major questions open, which we intend to solve by introducing ZüNIS, a fully automated NIS library. We first show how to extend the original formulation of NIS to reuse samples over multiple gradient steps, yielding a significant improvement for slow functions. We then benchmark ZüNIS over a range of problems and show high performance with limited fine-tuning. The library can be used by non-experts with minimal effort, which is crucial to become a mature tool for the wider HEP public.

1 INTRODUCTION

High-Energy-Physics (HEP) simulations are at the heart of the Large Hadron Collider (LHC) program for studying the fundamental laws of nature. Most HEP predictins are expressed as expectation values, evaluated numerically as Monte Carlo (MC) integrals. This permits both the integration of the very complex functions and the reproduction of the data selection process by experiments.

Most HEP simulations tools (Alwall et al., 2014) perform MC integrals using importance sampling, which allows to adaptively sample points to speed up convergence while keeping independent and identically distributed samples, crucial to reproduce experimental analyses which can only ingest uniformly-weighted data, typically produced by rejection sampling (see appendix A).

The most popular tool to optimize importance sampling is by far the VEGAS algorithm (Lepage, 1980; 2021), which fights the curse of dimensionality by assuming no correlations between the variables. While this is rarely the case in general, a good understanding of the integrand function can help significantly. Indeed optimized parametrizations using multichannelling (Kleiss et al., 1986; Ohl, 1999; Kleiss & Pittau, 1994) have become bread-and-butter tools for HEP event generation simulators, with good success for leading-order (LO) calculations. However, as simulations get more complex, either by having more complex final states or by including higher orders in perturbation theory, performance degrades fast.

There is much room for investing computational time into improving sampling (ATLAS Collaboration, 2020): modern HEP theoretical calculations are taking epic proportions and can require hours for a single function evaluation (Jones, 2018). Furthermore, unweighting samples can be extremely inefficient, with upwards of 90% sampled points discarded (Foundation et al., 2020). More powerful importance sampling algorithms would therefore be a welcome improvement (Buckley, 2020; WG et al., 2021).

First attempts to use machine learning (ML) to address this challenge explored using classical neural networks to sample (Bendavid, 2017; Klimek & Perelstein, 2020; Chen et al., 2021) but typically suffer from excessive computational costs. Another avenue of research has been to leverage generative models successful in other fields such as generative adversarial networks (Butter et al., 2019; Di Sipio et al., 2019; Butter et al., 2020; Ahdida et al., 2019; Hashemi et al., 2019; Carrazza & Dreyer, 2019). While such approaches do improve sampling speed by a large factor, they have ma-

jor limitations. In particular, they have no theoretical guarantees of providing a correct answer on average (Matchev et al., 2021) and poor control of uncertainties.

To avoid these disadvantages, our work exploits Neural Importance Sampling (NIS) (Müller et al., 2019; Zheng & Zwicker, 2019), which relies on normalizing flows and has strong theoretical guarantees.

A number of exploratory papers have been published on using NIS for LHC simulations (Gao et al., 2020b; Bothmann et al., 2020; Gao et al., 2020a), as well as closely related variations (Bellagente et al., 2021; Stienen & Verheyen, 2021), but most studies have focused on preliminary investigation of performance without much concern for the practical usability of the method. Indeed, training requires function evaluations, which we are trying to minimize and data-efficiency training is therefore an important but under-appreciated concern. Furthermore, few authors have provided usable open source code, making the adoption of the technique in the HEP community difficult.

As a result, we introduce ZÜNIS, a `PyTorch`-based library providing robust and usable NIS, usable by non-experts. We show that NIS is not only performant but can be formulated in a way that maximizes the use of a given function-evaluation budget. Not only does this optimize training, but this allows for cheap hyperparmeter tuning by reusing sampled data. ZÜNIS is flexible and extendable and provides multiple training strategies so that experts can fine-tune it to their needs, thanks to a detailed documentation.

2 Background

2.1 Importance sampling as an optimization problem

Importance sampling relies on the interpretation of integrals as expectation values. Indeed, let us consider an integral over a finite volume:

$$I = \int_\Omega dx f(x), \quad \text{where } V(\Omega) = \int_\Omega dx \text{ is finite.} \tag{1}$$

Let p be a strictly positive probability distribution over Ω, we can re-express our integral as an expectation value

$$I = \int_\Omega p(x) dx \frac{f(x)}{p(x)} = \mathop{\mathbb{E}}_{x\sim p}\left(\frac{f(x)}{p(x)}\right), \tag{2}$$

which motivates the introduction of a new estimator:

$$\hat{I}_N^p = \frac{1}{N}\sum_{i=1}^{N} \frac{f(X_i)}{p(X_i)}, \qquad X_i \sim p, \tag{3}$$

whose mean is indeed I and whose standard deviation is $\frac{\sigma(f,p)}{\sqrt{N}}$, where $\sigma(f,p)$ is the standard deviation of $f(X)/p(X)$ for $X \sim p$:

$$\sigma^2(f,p) = \mathop{\mathbb{E}}_{x\sim p}\left(\left(\frac{f(x)}{p(x)}\right)^2\right) - I^2. \tag{4}$$

The problem statement of importance sampling is to find the probability distribution function p that minimizes the variance of our estimator for a given N.

One can show that the minimum is obtained for $p(x) \propto |f(x)|$ (see appendix E). [1] This exact solution is however of no use in practice because there is in general no efficient way to sample from $|f|$.

Instead of relying on the exact solution, we therefore need to find an approximate solution *from a family of functions from which we can efficiently sample*. All importance sampling algorithms provide such a family and an optimization procedure to select the best candidate. In Neural Importance Sampling, we rely on Normalizing Flows, which we can optimize using stochastic gradient descent, as we shall discuss in the following section.

[1] If f is strictly positive, $f/|f|$ is constant and our estimator therefore has variance zero!

2.2 NORMALIZING FLOWS AND COUPLING CELLS

Normalizing flows (Tabak & Vanden-Eijnden, 2010; Tabak & Turner, 2013; Rippel & Adams, 2013; Rezende & Mohamed, 2015) provide a way to generate complex probability distribution functions from simpler ones using parametric changes of variables that can be learned to approximate a target distribution. As such, normalizing flows are diffeomorphisms: invertible, (nearly-everywhere) differentiable mappings with a differentiable inverse.

Let us start by restating the basics of the approach, and consider open sets $A, \Omega \subset R^n$. A diffeomorphism $T: A \to \Omega$ not only maps points through the relation $x = T(u)$ for $u \in A$, $x \in \Omega$, but also probability distribution functions: for every PDF p over A, there is a PDF q on Ω such that, if $u \sim p(u)$, $T(u) = x \sim q(x)$. The induced PDF q is expressed as

$$q\left(x = T(u)\right) = p(u)\left|J_T(u)\right|^{-1}, \tag{5}$$

where J_T is the Jacobian determinant of T:

$$J_T(u) = \det \frac{\partial T_i}{\partial u_j}(u). \tag{6}$$

In the world of machine learning, T is called a normalizing flow and is typically part of a parametric family of diffeomorphisms $(T(\cdot, \theta))$ such that gradients $\nabla_\theta J_T$ are tractable.

A necessary condition for this approach is the existence of families of diffeomorphisms with tractable Jacobians that can be optimized over. Coupling cell mappings perfectly satisfy this requirement (Dinh et al., 2015; 2017; Müller et al., 2018): they are neural-network-parametrized bijections whose Jacobian factor can be obtained analytically without backpropagation or expensive determinant calculation. As such, they provide a good candidate for importance sampling as long as they can be trained to learn an unnormalized target function, which is exactly what neural importance sampling proposes.

2.3 NEURAL IMPORTANCE SAMPLING

Neural importance sampling was introduced in the context of computer graphics (Müller et al., 2018) and proposes to use normalizing flows as a family of probability distributions over which to solve the minimization problem of importance sampling.

$$\mathcal{L}(\theta) = \int_\Omega \frac{f^2(x)}{p\left(x, \theta\right)}. \tag{7}$$

Of course, to actually do so, one needs to find a way to explicitly evaluate $\mathcal{L}(\theta)$ and the original neural importance sampling approach proposes to approximate it using importance sampling. One needs to be careful that the gradient of the estimator of the loss need not be the estimator of the gradient of the loss. The gradient of the loss can be expressed as

$$\nabla_\theta \mathcal{L}(\theta) = -\int_\Omega \frac{f^2(x)}{p\left(x, \theta\right)} \nabla_\theta \log p\left(x, \theta\right), \tag{8}$$

for which an estimator is proposed as

$$\widehat{\nabla}_\theta \mathcal{L}(\theta) = -\sum_{i=0}^{N} \left(\frac{f(X_i)}{p\left(X_i, \theta\right)}\right)^2 \nabla_\theta \log p\left(X_i, \theta\right), \quad X_i \sim p. \tag{9}$$

The authors also observed that other loss functions are possible which share the same global minimum as the variance based loss: for example, the Kullback-Leibler divergence D_{KL} between two functions is also minimized when they are equal. Such alternative loss functions are not guaranteed to work for importance sampling, but they prove quite successful in practice. After training to minimize the loss estimator of eq. (9), the normalizing flows provides a tractable probability distribution function from which to sample points and estimate the integral.

3 THE ZÜNIS FRAMEWORK: CONCEPTS AND ALGORITHMS

In this section we give a high-level overview of the organization of the ZÜNIS library and the algorithms it uses for importance sampling. The major conceptual innovation we provide in ZÜNIS is a more flexible and data-efficient way of training normalizing flows in the context of importance sampling. This relies on a more rigorous formulation of the connection between the theoretical expression of ideal loss functions in terms of integrals and their practical realizations as random estimators than in previous literature. We describe this improvement in section 3.2.

3.1 THE ZÜNIS LIBRARY

On the practical side, ZÜNIS is a `PyTorch`-based library which implements many ideas formulated in previous work but organizes them in the form of a modular software library with an easy-to-use interface and well-defined building blocks. We believe this structure will help non-specialist use it without understanding all the nuts and bolts, while experts can easily add new features to responds to their needs. The ZÜNIS library relies on three layers of abstractions which steer the different aspects of using normalizing flows to learn probability distributions from un-normalized functions and compute their integrals:

- `Flows`, which implement a bijective mapping which transforms points and computes the corresponding Jacobian are described in appendix F.1
- `Trainers`, which provide the infrastructure to perform training steps and sample from flow models are described in appendix F.2
- `Integrators`, which use trainers to steer the training of a model and compute integrals are described in appendix F.3

3.2 EFFICIENT TRAINING FOR IMPORTANCE SAMPLING

In this section, we describe how we train probability distributions within ZÜNIS using gradient-based optimizers. We want to find which member $p(x, \theta)$ of a parametric family of probability distribution functions minimizes eq. (7), which is also an integral we need to estimate. We will therefore define an auxiliary probability distribution function $q(x)$, independent from θ, from which we sample to estimate or loss function:

$$\int dx \frac{f(x)^2}{p(x,\theta)} = \mathop{\mathbb{E}}_{x\sim q} \frac{f(x)^2}{p(x,\theta)q(x)}. \tag{10}$$

This is the basis for the general method we use for training probability distributions within ZÜNIS, described in algorithm 1. Because the sampling distribution is separated from the model to train, the same point sample can be reused for multiple training steps, which is not possible when using eq. (9). This is particularly important for high-precision particle physics predictions that involve high-order perturbative calculations or complex detector simulations because function evaluations can be extremely costly.

From which distribution q should we sample for our loss estimation? Without any information on our function, a simple choice is to sample uniformly. Another possible approach is to use the information gathered during training, while respecting the constraint that $\nabla_\theta q(x) = 0$. To this end, we can take inspiration from deep Q-learning in which two copies of the models are used: one is trained using gradient-based optimization and is used to evaluate PDF values while the other is used for sampling and has its parameters frozen except for infrequent updates.

4 PERFORMANCE ASSESSMENT

In this section, we evaluate ZÜNIS on a variety of test functions to assess its performance and compare it to the commonly used VEGAS algorithm (Peter Lepage, 1978; Ohl, 1999). We first produce a few low dimensional examples for illustrative purposes, then move on to integrating parametric functions in various dimensions and finally evaluate performance on particle scattering matrix elements.

4.1 LOW-DIMENSIONAL EXAMPLES

Let us start by illustrating the effectiveness of ZÜNIS in a low dimensional setting where we can readily visualize results. We define three functions over the two dimensional hypercube:

$$f_{\text{camel}}(x) = \exp\left(-\left(\frac{x-\mu_1)}{\sigma}\right)^2\right) + \exp\left(-\left(\frac{x-\mu_2)}{\sigma}\right)^2\right), \tag{11}$$

$$f_{\varnothing}(x) = \min\left[1,\ \exp\left(-\left(\frac{|x|-r}{\sigma_{\varnothing}}\right)^2\right) + \exp\left(-\left(\frac{a\cdot x}{\sigma_{\varnothing}}\right)^2\right)\right] \tag{12}$$

$$f_{\sin}(x) = \cos\left(k\cdot x\right)^2, \tag{13}$$

to which we refer respectively as the camel, slashed circle and sinusoidal target functions. We set their parameters as follows

$$\mu_1 = \begin{pmatrix}0.25\\0.25\end{pmatrix},\ \mu_2 = \begin{pmatrix}0.75\\0.75\end{pmatrix},\ a = \begin{pmatrix}1\\-1\end{pmatrix},\ k = \begin{pmatrix}6\\6\end{pmatrix},\ \sigma = 0.1,\ \sigma_{\varnothing} = 0.1,\ r = 0.3 \tag{14}$$

We chose these functions because they illustrate different failure modes of the VEGAS algorithm (see appendix C).

We ran the ZÜNIS `Integrator` with default arguments over ten repetitions for each function and report the performance of the trained integral estimator compared to a flat estimator and to VEGAS in table 1. Overall, ZÜNIS `Integrators` learn to sample from their target function extremely well: we outperform VEGAS by a factor 100 for the camel and the slashed circle functions and a factor 30 for the sinusoidal function and VEGAS itself provides no advantage over uniform sampling for the latter two.

Variance Reduction	Camel	Slashed Circle	Sinusoidal
vs. uniform	$1.8 \pm 0.4 \times 10^3$	$8.9 \pm 0.9 \times 10^1$	$2.0 \pm 0.5 \times 10^2$
vs. VEGAS	$7.0 \pm 1.4 \times 10^2$	$8.8 \pm 0.9 \times 10^1$	$1.6 \pm 0.5 \times 10^2$

Table 1: Variance reduction (high is good) for the camel, slashed circle and sinusoidal functions compared to uniform sampling and to VEGAS over 10 repetitions.

We further illustrate the performance of our trained models by comparing the target functions and density histogram for points sampled from the normalizing flows in fig. 1, which shows great qualitative agreement.

4.2 SYSTEMATIC BENCHMARKS

Let us now take a more systematic approach to benchmarking ZÜNIS. We compare ZÜNIS Integrators against uniform integration and VEGAS using the following three metrics:

- integrand variance: this is a measure of the quality of the learned random variable sampler (section 2.1)
- unweighting efficiency: this is a measure of how efficient the learned sampler is for generating i.i.d data with rejection sampling as defined in appendix A
- training time: this is a measure of wall-clock time need to complete training[2].
- sampling time: a measure of wall-clock time per sampled point[2].

For this experiment, we focus on the camel function defined in eq. (11) and scan a variety of settings and dimensions. We always set the two peaks on the hyperdiagonal and span from 2 to 32 dimensions over function variances between 10^{-2} and 10^2 as shown in table 3.

[2]We provide details on hardware in appendix G

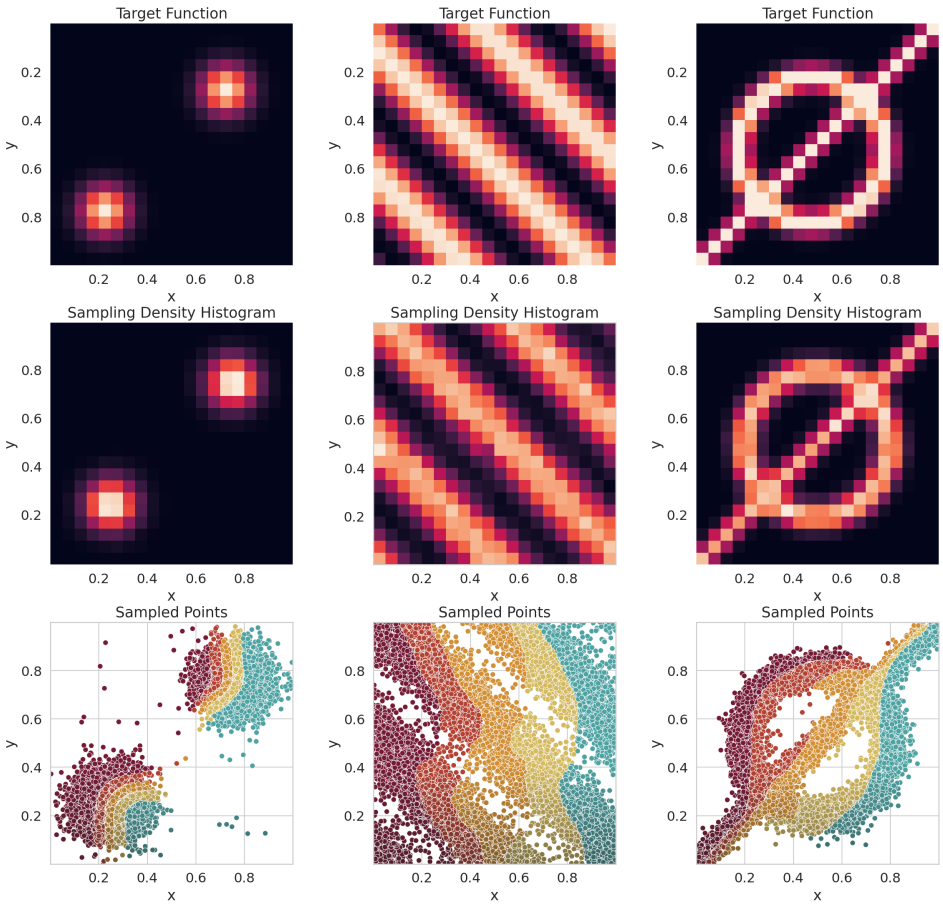

(a) Camel function (b) Sinusoidal function (c) Slashed circle function

Figure 1: Comparison between target functions and point sampling densities for 1a the camel function, 1b the sinusoidal function, 1c the slashed circle function. Supplementary fig. 7 shows how points are mapped from latent to target space.

We first test ZÜNIS by employing the default configuration over the 35 camel functions defined in table 3 to show the solid improvement `Integrators` provide over alternative approaches without any parameter tuning. Except in the low variance limit, ZÜNIS can reduce the required number of points sampled to attain a given precision on integral estimates, attaining speed-ups of up to $\times 1000$ both compared to uniform sampling and VEGAS-based importance sampling, as shown in fig. 2a-2b and table 4. Unweighting efficiencies are also boosted significantly, although more mildly than variances, as shown in fig. 2c-2d, which we could attribute to PDF underestimation in regions with low point density; the nature of the veto algorithm makes it very sensitive to a few bad behaving points in the whole dataset.

ZÜNIS does not, however, outclass VEGAS on all metrics by far: as shown in fig. 2, training is a few hundred times slower than VEGAS and sampling is 10-50 times slower, all while ZÜNIS runs on GPUs. This is to be expected given the much increased computational complexity of normalizing flows compared to the VEGAS algorithm. As such, ZÜNIS is not a general replacement for VEGAS, but provides a clear advantage for integrating time-intensive functions, where sampling is a negligible overhead, such as precision high-energy-physics simulations.

We have shown that ZÜNIS is a very performant importance sampling and event generation tool and provides significant improvements over existing tools, while requiring little fine tuning from users. Another key result is that the new approach to training we introduced in section 3.2 has a large positive impact on performance. Indeed, as we show in fig. 2, re-using samples for training

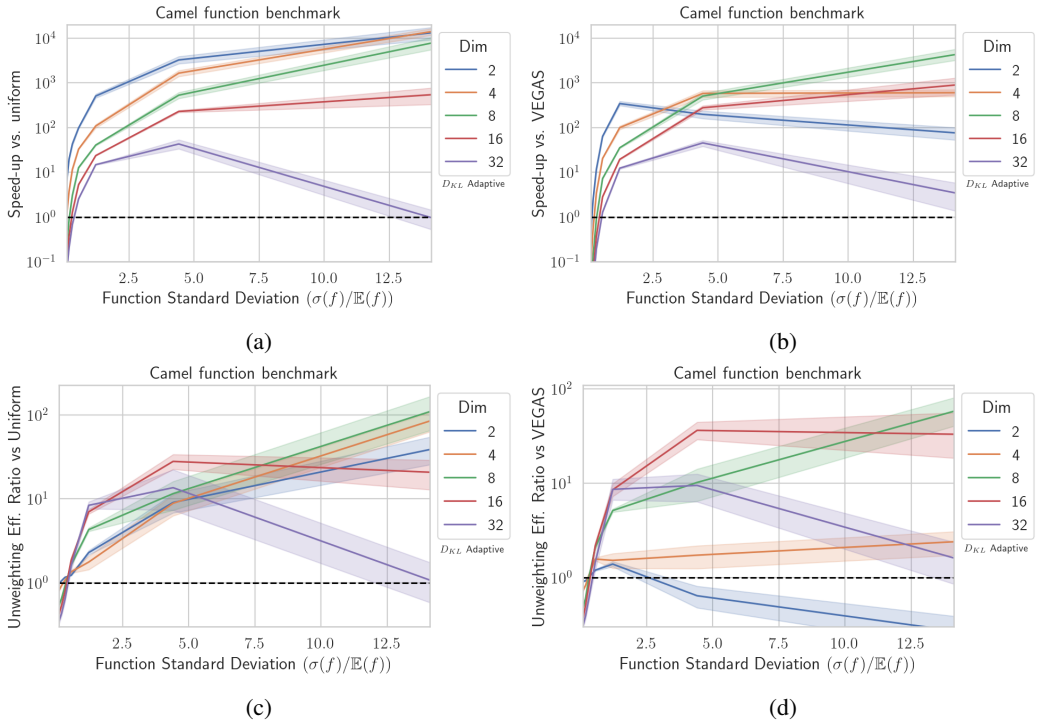

Figure 2: Benchmarking ZÜNIS against uniform sampling and VEGAS with default settings. In (2a-2b), we show the sampling speed-up (ratio of integrand variance) as a function of the relative standard deviation of the integrand, while we show the unweighting speed-up (ratio of unweighting efficiencies) in (2c-2d).

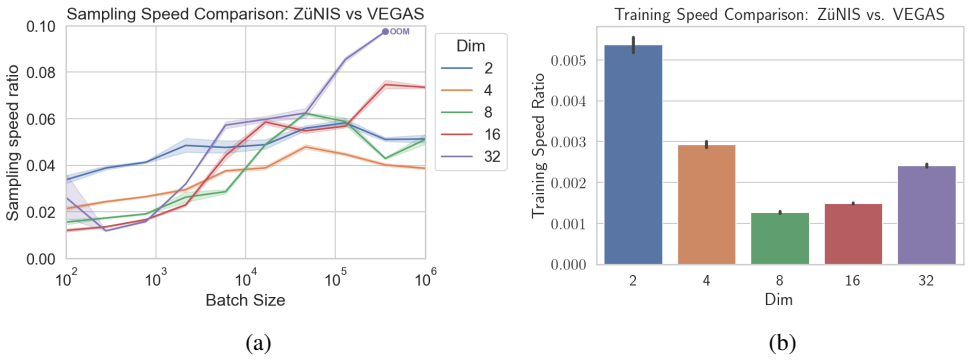

Figure 3: Comparison of the training and sampling speed of ZÜNIS and VEGAS. As can be expected, ZÜNIS is much slower than VEGAS, both for training and sampling, although larger batch sizes can better leverage the power of hardware accelerators.

over multiple epochs provides a 2- to 10-fold increase in convergence speed, making training much more data-efficient.

4.3 MADGRAPH CROSS SECTION INTEGRALS

Cross-sections are integrals of quantum transition matrix elements for a a scattering process such as a LHC collision and express the probability that specific particles are produced. Matrix elements themselves are un-normalized probability distributions for the configuration of the outgoing particles: it is therefore both valuable to integrate them to know the overall frequency of a given

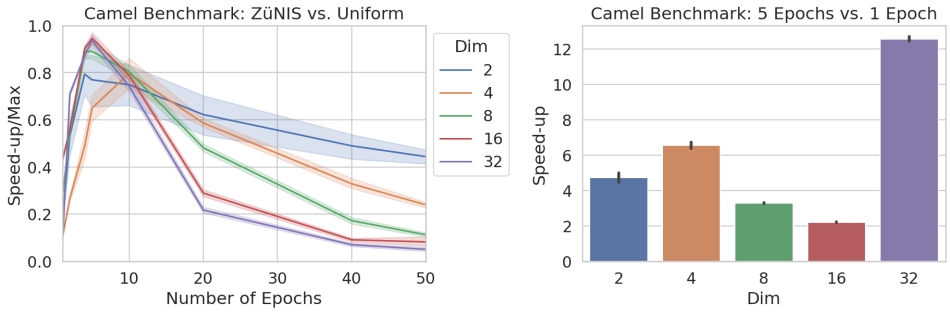

(a) (b)

Figure 4: Effect of repeatedly training on the same sample of points over multiple epochs. For all settings, there is a large improvement when going from one to moderate epoch counts, with a peak around 5-10. Larger number of epochs lead to overfitting, which impacts performance negatively.

scattering process, and to sample from them to understand how particles will be spatially distributed as they fly off the collision point.

We study the performance of ZÜNIS in comparison to VEGAS by studying three simple processes at leading order in perturbation theory, $e^-\mu \to e^-\mu$ via Z, $d\bar{d} \to d\bar{d}$ via Z and $uc \to ucg$ (with 3-jet cuts based on ΔR), see table 2 and fig. 5. We use the first process as a very easy reference while the two other, quark-initiated processes are used to illustrate specific points. Indeed, both feature narrow regions of their integration space with large enhancements, due respectively to Z-boson resonances and infra-red divergences.

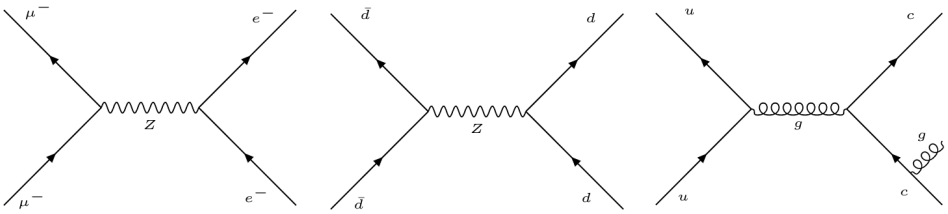

(a) (b) (c)

Figure 5: Sample Feynman Diagrams for $e^-\mu \to e^-\mu$ via Z, $d\bar{d} \to d\bar{d}$ via Z and $uc \to ucg$.

	$e^-\mu \to e^-\mu$ via Z	$d\bar{d} \to d\bar{d}$ via Z	$uc \to ucg$
dimensions	2	4	7
normalized standard deviation	1.45×10^{-2}	6.57×10^{-2}	0.96

Table 2: Comparison of the three test processes.

We evaluate the matrix elements for these three processes by using the FORTRAN standalone interface of MADGRAPH5_AMC@NLO (Alwall et al., 2014). The two hadronic processes are convolved with parton-distribution functions from `LHAPDF6` (Buckley et al., 2015). We parametrize phase space (the particle configuration space) using the RAMBO on diet algorithm (Plätzer, 2013) implemented for `PyTorch` in TORCHPS (Götz, 2021).

We report benchmark results in 6, in which we trained over 500,000 points for each process using near-default configuration, scanning only over variance and Kullback-Leibler losses.

We confirm our previous finding that processes with very small variance like $e^-\mu \to e^-\mu$, no integral convergence acceleration is achieved, but find however that ZÜNIS improves unweighting even in this situation. The two hadronic processes illustrate features we have observed when integrating

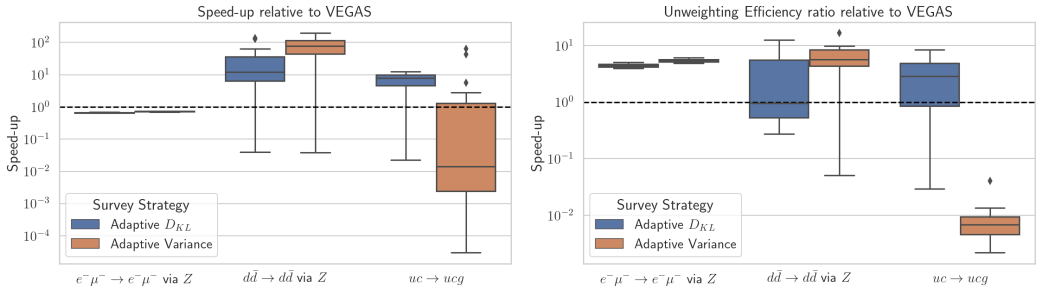

(a) (b)

Figure 6: Average performance of ZÜNIS over 20 runs relative to VEGAS, measured by the relative speed-up in 6a and by the relative unweighting efficiency in 6b.

cross sections: there is a large stochasticity of training and different processes are optimized by different loss function choices[3].

The performance of $d\bar{d} \to d\bar{d}$ shows nice improvement with ZÜNIS while that of $uc \to ucg$ is more limited. This is actually quite natural to understand when one compares performance against uniform sampling (see appendix D.3): it is in fact VEGAS, which performs significantly better on $uc \to ucg$ compared to $d\bar{d} \to d\bar{d}$ because the parametrization of RAMBO is based on splitting invariant masses, making them aligned with the enhancements in the ucg phase space and allowing great VEGAS performance. This drives a key conclusion for the potential role of ZÜNIS in the HEP simulation landscape: not to replace VEGAS, but to fill in the gaps where it fails due to inadequate parametrizations, as we illustrate here by using non-multichanneled $d\bar{d} \to d\bar{d}$ as a proxy for more complex processes.

5 Conclusion

We have showed that ZÜNIS can outperform VEGAS both in terms of integral convergence rate and unweighting efficiency on specific cases, at the cost of a significant increase in training and sampling time, which is an acceptable tradeoff for high-precision HEP computations with high costs. In this context, the introduction of efficient training is a key element to making the most of the power of neural importance sampling where function evaluation costs are a major concern. While further testing is required to ascertain how far NIS can fill the gaps left by VEGAS for integrating complex functions, there is already good evidence that ZÜNIS can provide needed improvements in specific cases. We hope that the publication of a usable toolbox for NIS such as ZÜNIS will stir a wider audience within the HEP community to apply the method so that the exact boundaries its applicability can be more clearly ascertained.

6 Reproducibility Statement

An anonymized version of the library is available on Github. The code itself can be installed through `PyPI` using `pip install zunis`. The data to reproduce the experiments can be generated using scripts provided in the repository at `experiments/benchmarks`, in which `Jupyter` notebooks are also available to reproduce the figures of the paper. The following scripts are available:

- `benchmarks_03/camel/run_benchmark_defaults.sh` to generate camel integration data
- `benchmarks_04/camel/run_benchmark_defaults.sh` to generate camel sampling speed data

[3]Generally, smoother functions are better optimized with the Kullback-Leibler loss while functions with peaks benefit from using the variance loss. As we show in D.4, choosing an adaptive strategy is generally advisable whatever the loss

- `benchmark_madgraph/ex_benchmark_emu.sh` to generate $e^-\mu \to e^-\mu$ via Z integration data
- `benchmark_madgraph/ex_benchmark_dd.sh` to generate $d\bar{d} \to d\bar{d}$ via Zintegration data
- `benchmark_madgraph/ex_benchmark_ucg.sh` to generate $uc \to ucg$ integration data

REFERENCES

C. Ahdida, R. Albanese, A. Alexandrov, A. Anokhina, S. Aoki, G. Arduini, E. Atkin, N. Azorskiy, J.J. Back, A. Bagulya, and et al. Fast simulation of muons produced at the ship experiment using generative adversarial networks. *Journal of Instrumentation*, 14(11):P11028–P11028, Nov 2019. ISSN 1748-0221. doi: 10.1088/1748-0221/14/11/p11028. URL http://dx.doi.org/10.1088/1748-0221/14/11/P11028.

J. Alwall, R. Frederix, S. Frixione, V. Hirschi, F. Maltoni, O. Mattelaer, H.-S. Shao, T. Stelzer, P. Torrielli, and M. Zaro. The automated computation of tree-level and next-to-leading order differential cross sections, and their matching to parton shower simulations. *Journal of High Energy Physics*, 2014(7), Jul 2014. ISSN 1029-8479. doi: 10.1007/jhep07(2014)079. URL http://dx.doi.org/10.1007/JHEP07(2014)079.

The ATLAS Collaboration. ATLAS HL-LHC Computing Conceptual Design Report. 2020.

Marco Bellagente, Manuel Haußmann, Michel Luchmann, and Tilman Plehn. Understanding Event-Generation Networks via Uncertainties. *arXiv:2104.04543 [hep-ph]*, April 2021.

Joshua Bendavid. Efficient Monte Carlo Integration Using Boosted Decision Trees and Generative Deep Neural Networks. 2017.

Enrico Bothmann, Timo Janßen, Max Knobbe, Tobias Schmale, and Steffen Schumann. Exploring phase space with Neural Importance Sampling. *SciPost Physics*, 8(4):069, April 2020. ISSN 2542-4653. doi: 10.21468/SciPostPhys.8.4.069.

Johann Brehmer and Kyle Cranmer. Flows for simultaneous manifold learning and density estimation. 2020.

Andy Buckley. Computational challenges for MC event generation. *Journal of Physics: Conference Series*, 1525:012023, April 2020. ISSN 1742-6596. doi: 10.1088/1742-6596/1525/1/012023.

Andy Buckley, James Ferrando, Stephen Lloyd, Karl Nordström, Ben Page, Martin Rüfenacht, Marek Schönherr, and Graeme Watt. LHAPDF6: parton density access in the LHC precision era. *The European Physical Journal C*, 75(3), Mar 2015. ISSN 1434-6052. doi: 10.1140/epjc/s10052-015-3318-8. URL http://dx.doi.org/10.1140/epjc/s10052-015-3318-8.

Anja Butter, Tilman Plehn, and Ramon Winterhalder. How to gan lhc events. *SciPost Physics*, 7 (6), Dec 2019. ISSN 2542-4653. doi: 10.21468/scipostphys.7.6.075. URL http://dx.doi.org/10.21468/SciPostPhys.7.6.075.

Anja Butter, Tilman Plehn, and Ramon Winterhalder. How to gan event subtraction. *SciPost Physics Core*, 3(2), Nov 2020. ISSN 2666-9366. doi: 10.21468/scipostphyscore.3.2.009. URL http://dx.doi.org/10.21468/SciPostPhysCore.3.2.009.

Stefano Carrazza and Frédéric A. Dreyer. Lund jet images from generative and cycle-consistent adversarial networks. *The European Physical Journal C*, 79(11), Nov 2019. ISSN 1434-6052. doi: 10.1140/epjc/s10052-019-7501-1. URL http://dx.doi.org/10.1140/epjc/s10052-019-7501-1.

I.-Kai Chen, Matthew D. Klimek, and Maxim Perelstein. Improved Neural Network Monte Carlo Simulation. *SciPost Physics*, 10(1):023, January 2021. ISSN 2542-4653. doi: 10.21468/SciPostPhys.10.1.023.

Riccardo Di Sipio, Michele Faucci Giannelli, Sana Ketabchi Haghighat, and Serena Palazzo. Dijetgan: a generative-adversarial network approach for the simulation of qcd dijet events at the lhc. *Journal of High Energy Physics*, 2019(8), Aug 2019. ISSN 1029-8479. doi: 10.1007/jhep08(2019)110. URL http://dx.doi.org/10.1007/JHEP08(2019)110.

Laurent Dinh, David Krueger, and Yoshua Bengio. NICE: Non-linear Independent Components Estimation, 2015.

Laurent Dinh, Jascha Sohl-Dickstein, and Samy Bengio. Density estimation using Real NVP, 2017.

HEP Software Foundation, Thea Aarrestad, Simone Amoroso, Markus Julian Atkinson, Joshua Bendavid, Tommaso Boccali, Andrea Bocci, Andy Buckley, Matteo Cacciari, Paolo Calafiura, Philippe Canal, Federico Carminati, Taylor Childers, Vitaliano Ciulli, Gloria Corti, Davide Costanzo, Justin Gage Dezoort, Caterina Doglioni, Javier Mauricio Duarte, Agnieszka Dziurda, Peter Elmer, Markus Elsing, V. Daniel Elvira, Giulio Eulisse, Javier Fernandez Menendez, Conor Fitzpatrick, Rikkert Frederix, Stefano Frixione, Krzysztof L. Genser, Andrei Gheata, Francesco Giuli, Vladimir V. Gligorov, Hadrien Benjamin Grasland, Heather Gray, Lindsey Gray, Alexander Grohsjean, Christian Gütschow, Stephan Hageboeck, Philip Coleman Harris, Benedikt Hegner, Lukas Heinrich, Burt Holzman, Walter Hopkins, Shih-Chieh Hsu, Stefan Höche, Philip James Ilten, Vladimir Ivantchenko, Chris Jones, Michel Jouvin, Teng Jian Khoo, Ivan Kisel, Kyle Knoepfel, Dmitri Konstantinov, Attila Krasznahorkay, Frank Krauss, Benjamin Edward Krikler, David Lange, Paul Laycock, Qiang Li, Kilian Lieret, Miaoyuan Liu, Vladimir Loncar, Leif Lönnblad, Fabio Maltoni, Michelangelo Mangano, Zachary Louis Marshall, Pere Mato, Olivier Mattelaer, Joshua Angus McFayden, Samuel Meehan, Alaettin Serhan Mete, Ben Morgan, Stephen Mrenna, Servesh Muralidharan, Ben Nachman, Mark S. Neubauer, Tobias Neumann, Jennifer Ngadiuba, Isobel Ojalvo, Kevin Pedro, Maurizio Perini, Danilo Piparo, Jim Pivarski, Simon Plätzer, Witold Pokorski, Adrian Alan Pol, Stefan Prestel, Alberto Ribon, Martin Ritter, Andrea Rizzi, Eduardo Rodrigues, Stefan Roiser, Holger Schulz, Markus Schulz, Marek Schönherr, Elizabeth Sexton-Kennedy, Frank Siegert, Andrzej Siódmok, Graeme A. Stewart, Malik Sudhir, Sioni Paris Summers, Savannah Jennifer Thais, Nhan Viet Tran, Andrea Valassi, Marc Verderi, Dorothea Vom Bruch, Gordon T. Watts, Torre Wenaus, and Efe Yazgan. HL-LHC Computing Review: Common Tools and Community Software. *arXiv:2008.13636 [hep-ex, physics:physics]*, August 2020. doi: 10.5281/zenodo.4009114.

Christina Gao, Stefan Höche, Joshua Isaacson, Claudius Krause, and Holger Schulz. Event generation with normalizing flows. *Physical Review D*, 101(7):076002, April 2020a. ISSN 2470-0010, 2470-0029. doi: 10.1103/PhysRevD.101.076002.

Christina Gao, Joshua Isaacson, and Claudius Krause. I-flow: High-dimensional Integration and Sampling with Normalizing Flows. *Machine Learning: Science and Technology*, 1(4):045023, November 2020b. ISSN 2632-2153. doi: 10.1088/2632-2153/abab62.

Niklas Götz. NGoetz/TorchPS:-v1.0.1, March 2021. URL https://doi.org/10.5281/zenodo.4639109. Available at https://github.com/NGoetz/TorchPS/tree/v1.0.1, version 1.0.1.

Bobak Hashemi, Nick Amin, Kaustuv Datta, Dominick Olivito, and Maurizio Pierini. Lhc analysis-specific datasets with generative adversarial networks, 2019.

F. James. Monte Carlo Theory and Practice. *Rept. Prog. Phys.*, 43:1145, 1980. doi: 10.1088/0034-4885/43/9/002.

S.P. Jones. Higgs Boson Pair Production: Monte Carlo Generator Interface and Parton Shower. *Acta Physica Polonica B Proceedings Supplement*, 11(2):295, 2018. ISSN 1899-2358, 2082-7865. doi: 10.5506/APhysPolBSupp.11.295.

R. Kleiss and R. Pittau. Weight optimization in multichannel Monte Carlo. *Computer Physics Communications*, 83(2-3):141–146, December 1994. ISSN 00104655. doi: 10.1016/0010-4655(94)90043-4.

R Kleiss, W. J Stirling, and S. D Ellis. A new Monte Carlo treatment of multiparticle phase space at high energies. *Computer Physics Communications*, 40(2):359–373, June 1986. ISSN 0010-4655. doi: 10.1016/0010-4655(86)90119-0.

Matthew Klimek and Maxim Perelstein. Neural network-based approach to phase space integration. *SciPost Physics*, 9(4):053, October 2020. ISSN 2542-4653. doi: 10.21468/SciPostPhys.9.4.053.

G. Peter Lepage. VEGAS: AN ADAPTIVE MULTIDIMENSIONAL INTEGRATION PROGRAM. March 1980.

G. Peter Lepage. Adaptive Multidimensional Integration: VEGAS Enhanced. *Journal of Computational Physics*, 439:110386, August 2021. ISSN 00219991. doi: 10.1016/j.jcp.2021.110386.

Konstantin T. Matchev, Alexander Roman, and Prasanth Shyamsundar. Uncertainties associated with GAN-generated datasets in high energy physics. *arXiv:2002.06307 [hep-ex, physics:hep-ph, physics:physics]*, June 2021.

Thomas Müller, Brian McWilliams, Fabrice Rousselle, Markus Gross, and Jan Novák. Neural Importance Sampling, 2018.

Thomas Müller, Brian Mcwilliams, Fabrice Rousselle, Markus Gross, and Jan Novák. Neural Importance Sampling. *ACM Transactions on Graphics*, 38(5):1–19, November 2019. ISSN 0730-0301, 1557-7368. doi: 10.1145/3341156.

Thorsten Ohl. Vegas revisited: Adaptive Monte Carlo integration beyond factorization. *Comput. Phys. Commun.*, 120:13–19, 1999. doi: 10.1016/S0010-4655(99)00209-X.

G Peter Lepage. A new algorithm for adaptive multidimensional integration. *Journal of Computational Physics*, 27(2):192–203, 1978. ISSN 0021-9991. doi: https://doi.org/10.1016/0021-9991(78)90004-9. URL https://www.sciencedirect.com/science/article/pii/0021999178900049.

Simon Plätzer. RAMBO on diet, 2013.

Danilo Jimenez Rezende and Shakir Mohamed. Variational inference with normalizing flows. *32nd International Conference on Machine Learning, ICML 2015*, 2:1530–1538, 2015. ISSN 9781510810587.

Oren Rippel and Ryan Prescott Adams. High-dimensional probability estimation with deep density models. *arXiv preprint arXiv:1302.5125*, 2013.

Bob Stienen and Rob Verheyen. Phase Space Sampling and Inference from Weighted Events with Autoregressive Flows. *SciPost Physics*, 10(2):038, February 2021. ISSN 2542-4653. doi: 10.21468/SciPostPhys.10.2.038.

Esteban G Tabak and Cristina V Turner. A family of nonparametric density estimation algorithms. *Communications on Pure and Applied Mathematics*, 66(2):145–164, 2013.

Esteban G Tabak and Eric Vanden-Eijnden. Density estimation by dual ascent of the log-likelihood. *Communications in Mathematical Sciences*, 8(1):217–233, 2010.

The HSF Physics Event Generator WG, Andrea Valassi, Efe Yazgan, Josh McFayden, Simone Amoroso, Joshua Bendavid, Andy Buckley, Matteo Cacciari, Taylor Childers, Vitaliano Ciulli, Rikkert Frederix, Stefano Frixione, Francesco Giuli, Alexander Grohsjean, Christian Gütschow, Stefan Höche, Walter Hopkins, Philip Ilten, Dmitri Konstantinov, Frank Krauss, Qiang Li, Leif Lönnblad, Fabio Maltoni, Michelangelo Mangano, Zach Marshall, Olivier Mattelaer, Javier Fernandez Menendez, Stephen Mrenna, Servesh Muralidharan, Tobias Neumann, Simon Plätzer, Stefan Prestel, Stefan Roiser, Marek Schönherr, Holger Schulz, Markus Schulz, Elizabeth Sexton-Kennedy, Frank Siegert, Andrzej Siódmok, and Graeme A. Stewart. Challenges in Monte Carlo event generator software for High-Luminosity LHC. *Computing and Software for Big Science*, 5 (1):12, December 2021. ISSN 2510-2036, 2510-2044. doi: 10.1007/s41781-021-00055-1.

Quan Zheng and Matthias Zwicker. Learning to Importance Sample in Primary Sample Space. *Computer Graphics Forum*, 38(2):169–179, 2019. ISSN 1467-8659. doi: 10.1111/cgf.13628.

A EVENT GENERATION WITH THE VETO ALGORITHM

Generating i.i.d points following an arbitrary probability distributions in high dimensions is not a priori a trivial task. A straightforward way to obtain such data is to use rejection sampling, which can be based on any distribution q from which we can sample. Given an i.i.d sample $x_1, \ldots, x_N \sim q$, we can define weights $w(x_i) = p(x_i)/q(x_i)$ and keep/reject points with probability $w(x_i)/w_{\text{max}}$.

The main metric for evaluating the performance of this algorithm is the unweighting efficiency: how much data is kept from an original sample of size N on average, which is expressed as

$$\epsilon_{\text{unw}} = \mathop{\mathbb{E}}_{x\sim q} \frac{w(x)}{w_{\text{max}}}. \tag{15}$$

B BACKWARD SAMPLING ALGORITHM

Algorithm 1: Backward sampling training in ZÜNIS

Data: Parametric PDF $p(x, \theta)$
Result: Trained PDF $p(x, \theta)$

```
for M steps do
    Sample a batch x_1, ..., x_{n_batch} from q;
    Compute the sampling PDF values q(x_i);
    Compute function values f(x_i);
    Start tracking gradients with respect to θ;
    for N steps do
        Compute the PDF values from the parametric PDF p(x_i, θ);
        Estimate the loss L̂ = (1/N) Σ_{i=1}^{n_batch} f(x_i)^2 / (p(x, θ) q(x));
        Compute ∇_θ L̂ using backpropagation;
        Set θ ← θ − η ∇_θ L̂;
        Reset gradients;
    end
end
return p(x, θ);
```

C FUNDAMENTAL LIMITATIONS OF THE VEGAS ALGORITHM

- Because of the factorized PDF of VEGAS, the camel function leads to 'phantom peaks' in the off diagonal. This problem grows exponentially with the number of dimensions but can be addressed by a change of variable to align the peaks with an axis of integration.
- The sinuoidal function makes it nearly impossible for VEGAS to provide any improvement: the marginal PDF over each variable of integration is nearly constant. Again this type of issue can be addressed by a change of variable provided one knows how to perform it.
- The slashed circle function is an example of a hard-for-VEGAS function that cannot be improved significantly by a change of variables. One can instead use multi-channeling, but this requires a lot of prior knowledge and has a computational costs since each channel is its own integral.

D SUPPLEMENTARY RESULTS

D.1 QUALITATIVE EXAMPLES

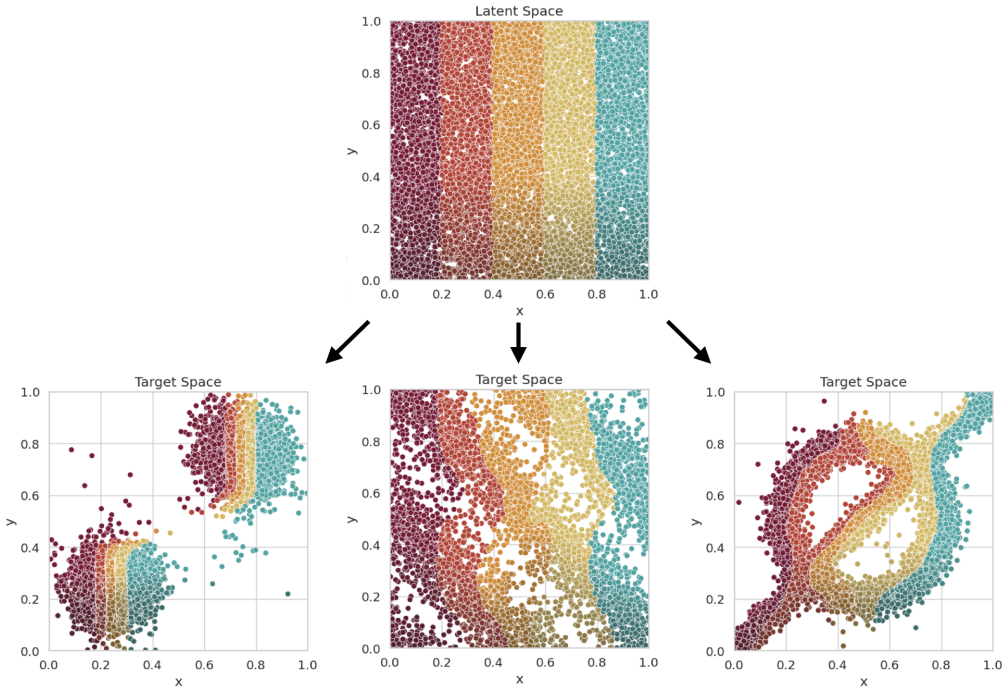

Figure 7: Mapping between the uniform point density in the latent space and the target distribution for the camel function, the sinusoidal function, the slashed circle function. Points are colored based on their position in latent space.

D.2 SYSTEMATIC BENCHMARK DETAILS

	Dimension					σ_{1d}	rel. st.d
	2	4	8	16	32		
Camel param. σ	2.00×10^{-2}	8.93×10^{-2}	2.04×10^{-1}	3.61×10^{-1}	5.06×10^{-1}	0.001	14.1
	6.32×10^{-2}	1.64×10^{-1}	3.14×10^{-1}	4.64×10^{-1}	6.06×10^{-1}	0.01	4.41
	2.21×10^{-1}	3.78×10^{-1}	5.23×10^{-1}	6.67×10^{-1}	8.25×10^{-1}	0.1	1.22
	4.51×10^{-1}	5.93×10^{-1}	7.43×10^{-1}	9.11×10^{-1}	1.10	0.3	0.56
	6.44×10^{-1}	7.99×10^{-1}	9.74×10^{-1}	1.18	1.41	0.5	0.32
	8.62×10^{-1}	1.05	1.26	1.51	1.81	0.7	0.19
	1.21	1.45	1.73	2.07	2.47	1.0	0.10

Table 3: Setup of the 35 different camel functions considered to benchmark ZÜNIS. We scan over function relative standard deviations, which correspond to different σ parameters for each dimension(eq. (11)). We provide the corresponding width of a 1D gaussian (σ_{1d}) with the same variance for reference.

	Dimension					σ_{1d}	rel. st.d
	2	4	8	16	32		
VEGAS speed-up	$7.6^{+2.4}_{-2.4} \times 10^1$	$6.0^{+1.2}_{-1.0} \times 10^2$	$4.3^{+1.4}_{-1.0} \times 10^3$	$9.0^{+4.7}_{-3.1} \times 10^2$	$3.5^{+2.7}_{-1.8} \times 10^0$	0.001	14.11
	$2.0^{+0.4}_{-0.4} \times 10^2$	$5.8^{+0.8}_{-1.0} \times 10^2$	$5.1^{+0.8}_{-0.9} \times 10^2$	$2.8^{+0.3}_{-0.3} \times 10^2$	$4.5^{+0.6}_{-0.8} \times 10^1$	0.01	4.41
	$3.4^{+0.5}_{-0.3} \times 10^2$	$1.0^{+0.1}_{-0.1} \times 10^2$	$3.5^{+0.1}_{-0.2} \times 10^1$	$1.9^{+0.1}_{-0.1} \times 10^1$	$1.2^{+0.1}_{-0.1} \times 10^1$	0.1	1.22
	$6.3^{+0.4}_{-0.3} \times 10^1$	$2.0^{+0.0}_{-0.1} \times 10^1$	$7.2^{+0.3}_{-0.3} \times 10^0$	$2.8^{+0.1}_{-0.1} \times 10^0$	$1.3^{+0.1}_{-0.0} \times 10^0$	0.3	0.56
	$1.2^{+0.1}_{-0.1} \times 10^1$	$3.5^{+0.1}_{-0.2} \times 10^0$	$9.1^{+0.6}_{-0.4} \times 10^{-1}$	$3.7^{+0.2}_{-0.2} \times 10^{-1}$	$2.0^{+0.1}_{-0.1} \times 10^{-1}$	0.5	0.33
	$2.4^{+0.2}_{-0.2} \times 10^0$	$5.3^{+0.5}_{-0.4} \times 10^{-1}$	$1.3^{+0.1}_{-0.1} \times 10^{-1}$	$5.5^{+0.4}_{-0.3} \times 10^{-2}$	$3.0^{+0.1}_{-0.2} \times 10^{-2}$	0.7	0.20
	$4.0^{+0.6}_{-0.5} \times 10^{-1}$	$7.8^{+0.6}_{-0.5} \times 10^{-2}$	$1.6^{+0.1}_{-0.1} \times 10^{-2}$	$7.8^{+0.8}_{-0.6} \times 10^{-3}$	$4.8^{+0.3}_{-0.4} \times 10^{-3}$	1.0	0.11

Table 4: Variance reduction factor compared to VEGAS for each of the 35 different camel setups defined in table 3.

D.3 COMPARING ZÜNIS WITH UNIFORM SAMPLING ON MATRIX ELEMENTS

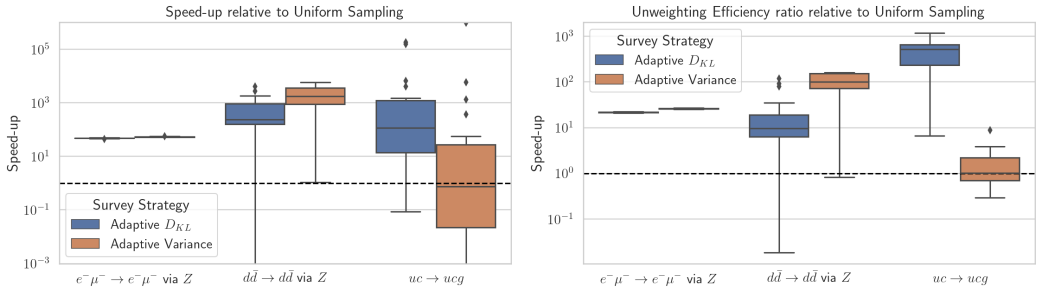

(a) (b)

Figure 8: Average performance of ZÜNIS over 20 runs relative to flat sampling, measured by the relative speed-up in 8a and by the relative unweighting efficiency in 8b.

D.4 EFFECT OF SURVEY STRATEGIES

In the following, we want to investigate how the integration of the three example processes in 4.3 with ZÜNIS behaves relative to VEGAS in dependence of the choice of the loss function, the survey strategy and the number of epochs during training. For all other options, the default values are chosen again, except for the number of points during the survey phase, which is set to 500,000.

Figure 9a shows that for a simple process like $e^-\mu \to e^-\mu$ via Z , where no correlations exist, ZÜNIS cannot reach the speed-up achieved by VEGAS. Variance loss seems to lead to higher variance improvements than D_{KL} loss. Contrary, 9b shows that ZÜNIS can greatly improve the unweighting efficiency for this process. The effect is again consistently stronger when using variance loss. Using a flat survey strategy suffers for both loss functions from overfitting, whereas adaptive sampling in average performs slightly better and does not show overfitting.

$d\bar{d} \to d\bar{d}$ via Z presents a more realistic use case, as the parton distribution functions introduce correlations between the integration variables which present a challenge to the VEGAS algorithm.

For this process, both the speed-up and the unweighting efficiency ratio clearly favor the variance loss again, which outperforms in both metrics the D_{KL} loss when multiple epochs are used. The richer structure of the integrand reduces the effect of overfitting. Therefore, the performance increases or stays approximately constant except for the combination of D_{KL} loss and the forward survey strategy. For the variance loss, it becomes apparent that the flat survey strategy increases much slower in performance than alternative strategies as a function of the number of epochs. However, for combination of losses and survey strategies, VEGAS could be outperformed substantially in terms of integration speed.

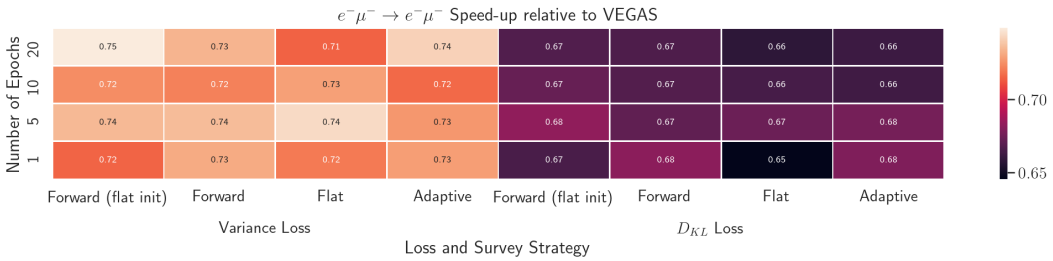

(a)

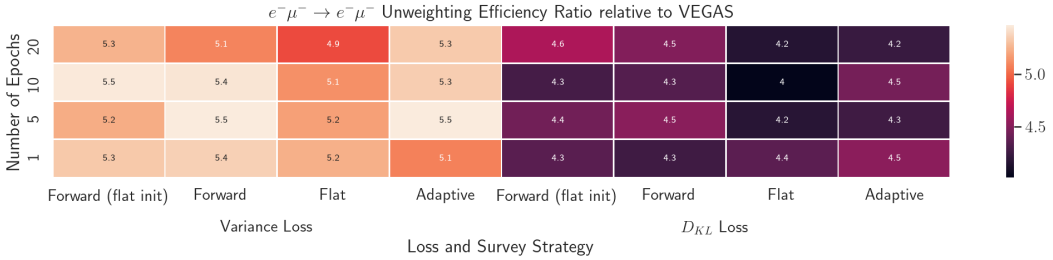

(b)

Figure 9: Median of the performance of ZÜNIS over 20 runs relative to VEGAS for the process $e^-\mu \to e^-\mu$ via Z depending on the loss function, the survey strategy and number of epochs, measured by the relative speed-up in 9a and by the relative unweighting efficiency in 9b.

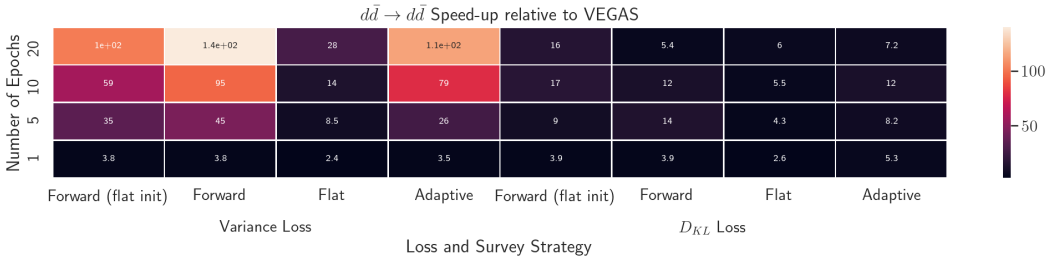

(a)

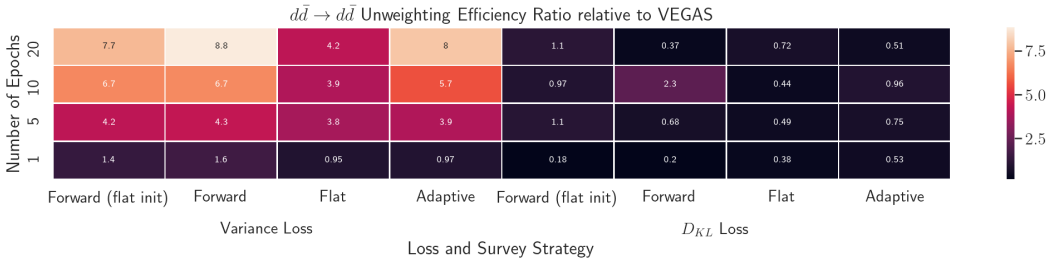

(b)

Figure 10: Median of the performance of ZÜNIS over 20 runs relative to VEGAS for the process $d\bar{d} \to d\bar{d}$ via Z depending on the loss function, the survey strategy and number of epochs, measured by the relative speed-up in 10a and by the relative unweighting efficiency in 10b.

An opposite picture is drawn by the process $uc \to ucg$ in figure 11, for which, apart from the flat survey strategy, D_{KL} loss is in general favored both for integration speed as well as unweighting efficiency ratio. The adaptive survey strategy is here giving the best results, although for a high number of epochs causes overfitting for the unweighting efficiency.

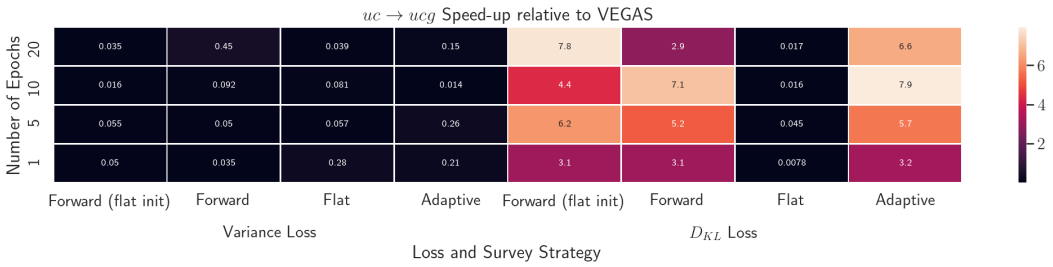

(a)

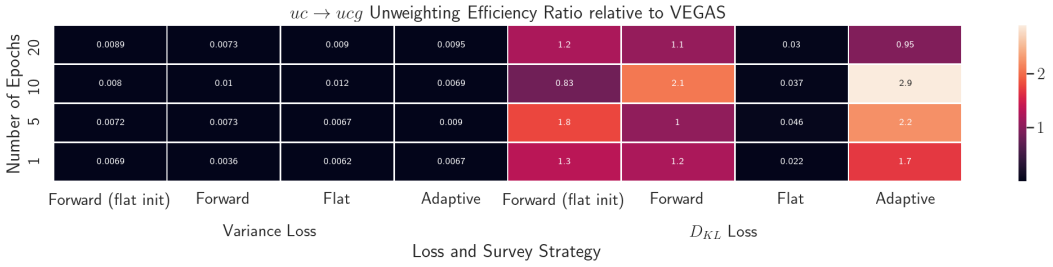

(b)

Figure 11: Median of the performance of ZÜNIS over 20 runs relative to VEGAS for the process $uc \to ucg$ depending on the loss function, the survey strategy and number of epochs, measured by the relative speed-up in 11a and by the relative unweighting efficiency in 11b.

The take-home message of this section is, one the one hand, that the flat survey strategy is in general not recommended. Apart from this, the most important mean to improve the quality of importance sampling are testing whether, independent of the survey strategy, the loss function should be chosen differently.

E Exact minimzation of the neural importance sampling estimator variance

Let us show that the optimal probability distribution for importance sampling is the function itself. Explicitly, as discussed in section 2.1, we want to find the probability distribution p defined over some domain Ω which minimizes the variance of the estimator $f(X)/p(X)$, for $X \sim p(X)$. We showed that this amounts to solving the following optimization problem:

$$\min_p \mathcal{L}(p) = \int_\Omega dx \frac{f(x)^2}{p(x)}, \quad \text{such that} \int dx\, p(x) = 1, \tag{16}$$

which we can encode using Lagrange multipliers

$$p = \arg\min \mathcal{L}(p, \lambda) = \int_\Omega dx \frac{f(x)^2}{p(x)} + \lambda \left(p(x) - \frac{1}{V(\Omega)} \right). \tag{17}$$

We can now solve this problem by finding extrema with functional derivatives

$$\frac{\delta \mathcal{L}(p, \lambda)}{\delta p(x)} = \lambda - \frac{f(x)^2}{p(x)^2}, \tag{18}$$

which indeed is zero if $p(x) \propto |f(x)|$. Furthermore, this extremum is certainly a minimum because the loss function is positive and unbounded. Indeed, if we separate Ω into two disjoint measurable subdomains Ω_1 and Ω_2, and define $p_\alpha(x)$ such that points are drawn uniformly over Ω_1 with probability α and uniformly over Ω_2 with probability $1 - \alpha$, then the resulting loss function would be

$$\mathcal{L}(p_\alpha) = \frac{V(\Omega_1)}{\alpha} \int_{\Omega_1} dx\, f(x)^2 + \frac{V(\Omega_2)}{1-\alpha} \int_{\Omega_2} dx\, f(x)^2, \tag{19}$$

which can be made arbitrarily large by sending α to 0.

F HIGH-LEVEL CONCEPTS OF THE ZÜNIS API

F.1 NORMALIZING FLOWS WITH FLOW CLASSES

Flows map batches of points and their densities. The ZÜNIS library implements normalizing flows by specifying a general interface defined as a Python abstract class: `GeneralFlow`. All flow models in ZÜNIS are child classes of `GeneralFlow`, which itself inherits from the Pytorch `nn.Module` interface.

As defined in section 2.2, a normalizing flow in ZÜNIS is a bijective mapping between two d dimensional spaces, which in practice are always the unit hypercube $[0,1]^d$ or $\mathbb{R}^d$, with a tractable Jacobian so that it can be used to map probability distributions. To this end, the `GeneralFlow` interface defines normalizing flows as a callable Python object which acts on batches of point drawn from a known PDF p. A batch of points x_i with their PDF values is encoded as a Pytorch `Tensor` object X organized as follows

$$X = (X_1, \ldots, X_{\text{batch}}) \in \mathbb{R}^{\text{batch}} \times \mathbb{R}^{d+1}, \tag{20}$$

where each X_i corresponds to a points stacked with its negative log density

$$X_i = \begin{pmatrix} x_{i,1} \\ \vdots \\ x_{i,d} \\ -\log p(x_i) \end{pmatrix}. \tag{21}$$

Encoding point densities by their negative logarithm makes their transformation under normalizing flows additive. Indeed if we have a mapping Q with Jacobian determinant j_Q, then $x \sim p(x)$ is mapped to $y = Q(x) \sim \tilde{p}(y)$ such that

$$-\log \tilde{p}(y) = -\log p(x) + \log j_Q(x). \tag{22}$$

Coupling Cells are flows defined by an element-wise transform and a mask. All flow models used in ZÜNIS in practice are implemented as a sequence of coupling cell transformations acting on a subset of the variables. The abstract class `GeneralCouplingCell` and its child `InvertibleCouplingCell` specifies the general organization of coupling cells as needing to be instantiated with

- a dimension d
- a mask defined as a list of boolean specifying which coordinates are transformed or not
- a transform that implements the mapping of the non-masked variables

In release v1.0 of ZÜNIS two such classes are provided: `PWLinearCoupling` and `PWQuadraticCoupling`, which respectively implement the piecewise linear and piecewise quadratic coupling cells proposed in (Müller et al., 2018). New coupling cells can easily be implemented, as explained in appendix F.4. Both existing classes rely on dense neural networks for the prediction of the shape of their one-dimensional piecewise-polynomial mappings, whose parameters are set at instantiation.

Here is how one can use a piecewise-linear coupling cell for sampling points

```
import torch
from zunis.models.flows.coupling_cells.piecewise_coupling.
    piecewise_quadratic import PWQuadraticCoupling
d=2
N_batch=10
mask = [True,False]
x = torch.zeros((N_batch,d+1))
# Sample the d first entries uniformly, keep 0. for the negative log
    jacobian
x[...,:-1].uniform_()
print(x[0]) # [0.3377, 0.4362, 0.]
f = PWQuadraticCoupling(d=d,mask=mask)
y = f(x)
print(y[0]) # [0.3377, 0.4411, -0.0314]
```

We provide further details of the use and possible parameters of flows in the documentation of ZÜNIS: https://zunis-anonymous.github.io/zunis/.

F.2 TRAINING WITH THE TRAINER CLASS

The design of the ZÜNIS library intentionally restricts `Flow` models to being bijective mappings instead of being ways to evaluate and sample from PDFs so as not to restrict their applicability (see Brehmer & Cranmer (2020) for an example). The specific application in which one uses a normalizing flow, and in our case how precisely one samples from it, is intimately linked to how such a model is trained. As a result, ZÜNIS bundles together the low-level training tools for `Flow` models together with sampling tools inside the `Trainer` classes.

The general blueprint for such classes is defined in the `GenericTrainerAPI` abstract class while the main implementation for users is provided as `StatefulTrainer`. At instantiation, all trainers expect a `Flow` model and `flow_prior` which samples point from a fixed PDF in latent space. These two elements together define a probability distribution over the target space from which one can sample.

There are two main ways one interacts with `Trainers`:

- One can sample points from the PDF defined by the model and the prior using the `sample_forward` method.
- One can train over a pre-sample batch of points, their sampling PDF and the corresponding function values using `train_on_batch(self, x, px, fx)`

In practice, we expect that the main way users will use `Trainers` is for sampling pre-trained models. In the context of particle physics simulations for example, *unweighting* is a common task, which aims at sampling exactly from a known function f. A common approach is the *Hit-or-miss* algorithm (James, 1980), whose efficiency is improved by sampling from a PDF approaching f. This is how one would use a trainer trained on f:

```
# [...]
# import or train a trainer `pretrained_trainer`
import torch

# Sampling points
xj = pretrained_trainer.sample_forward(100)
x = x[:, :-1]
px = (-x[:,-1]).exp()
fx = f(x)

# Applying the veto algorithm
fmax = fx.max()
veto = (fx/fmax - torch.zeros_like(fx).uniform_(0.,1.)) > 0.
x_unweighted = x[veto]
# x_unweighted follows the PDF obtained by normalizing f.
```

F.3 INTEGRATING WITH THE INTEGRATOR CLASS

Integrators are intended as the main way for standard users to interact with ZÜNIS. They provide a high-level interface to the functionalities of the library and only optionally require users to know to what lower levels of abstractions really entail and to what their options correspond. From a practical point of view, the main interface of ZÜNIS for integration is implemented as the `Integrator`, which is a factory function that instantiates the appropriate integrator class based on a choice of options.

All integrators follow the same pattern, defined in the `SurveyRefineIntegratorAPI` and `BaseIntegrator` abstract classes. Integration start by performing a survey phase, in which it optimizes the way it samples points and then a refine phase, in which it computes the integral by using its learned sampler. Each phase proceeds through a number of steps, which can be set at instantiation or when integrating:

```
# Setting values at instantiation time
integrator = Integrator(d=d, f=f, n_iter_survey=3, n_iter_refine=5)
# Override at integration time
integral_data = integrator.integrate(n_survey=10, n_refine=10)
```

For both the survey and the refine phases, using multiple steps is useful to monitor the stability of the training and of the integration process: if one step is not within a few standard deviations of the next, either the sampling statistics are too low, or something is wrong. For the refine stage, this is the main real advantage of using multiple steps. On the other hand, at each new survey step, a new batch of points is re-sampled, which can be useful to mitigate overfitting.

By default, only the integral estimates obtained during the refine stage are combined to compute the final integral estimate, and their combination is performed by taking their average. Indeed, because the model is trained during the survey step, the points sampled during the refine stage are correlated in an uncontrolled way with the points used during training. Ignoring the survey stage makes all estimates used in the combination independent random variables, which permits us to build a formally correct estimator of the variance of the final result.

F.4 Implementing new coupling cells

To implement a new invertible coupling cell inheriting from `InvertibleCouplingCell`, one must provide an `InvertibleTransform` object and define a callable attribute `T` computing the parameters of the transform. For example, consider a very simple linear coupling cell over $\mathbb{R}$

$$y = Q(x) : \begin{cases} y^A = x^A \\ y^B = \exp\left(T(x^A)\right) \times x^B, \end{cases} \tag{23}$$

where $T(x^A)$ is a scalar strictly positive value. This can be defined in the following way in ZÜNIS

```
import torch
from zunis.models.flows.coupling_cells.general_coupling import
    InvertibleCouplingCell
from zunis.models.flows.coupling_cells.transforms import
    InvertibleTransform
from zunis.models.layers.trainable import ArbitraryShapeRectangularDNN

class LinearTransform(InvertibleTransform):
   def forward(self,x,T):
      alpha = torch.exp(T)
      logj = T*x.shape[-1]
      return x*alpha, logj
   def backward(self,x,T):
      alpha = torch.exp(-T)
      logj = -T*x.shape[-1]
      return x*alpha, logj
```

```
class LinearCouplingCell(InvertibleCouplingCell):
   def __init__(self, d, mask, nn_width, nn_depth):
      transform = LinearTransform()
      super(LinearCouplingCell, self).__init__(d=d, mask=mask,transform=
          transform)
      d_in = sum(mask)
      self.T = ArbitraryShapeRectangularDNN(d_in=d_in,
                                            out_shape=(1,),
                                            d_hidden=nn_width,
                                            n_hidden=nn_depth)
```

G HARDWARE SETUP DETAILS

The computations presented in this work were performed on a computing cluster using a Intel(R) Xeon(R) Gold 5218 CPU @ 2.30GHz with 376 GB RAM. Processes which could be performed on the GPU were done on a GeForce RTX 2080 having 12 GB memory and running on CUDA 11.0.